PLOS ONE

RESEARCH ARTICLE

NGF Modulates trkA^{NGFR}/p75^{NTR} in αSMA-Expressing Conjunctival Fibroblasts from Human Ocular Cicatricial Pemphigoid (OCP)

Alessandra Micera[1☯]*, Barbara Stampachiacchiere[1☯], Antonio Di Zazzo[2], Roberto Sgrulletta[2], Magdalena Cortes[1], Eduardo Maria Normando[3,4], Alessandro Lambiase[5], Stefano Bonini[2]*

1 IRCCS-G.B. Bietti Foundation, Rome, Italy, **2** Department of Ophthalmology, University Campus Bio-Medico, Rome, Italy, **3** Glaucoma & Retinal Degeneration Research Group, Visual Neurosciences, UCL Institute of Ophthalmology, 11–43 Bath Street, London, EC1V 9EL, United Kingdom, **4** The Western Eye Hospital, Imperial College Healthcare Trust, Marylebone Road, London, NW1 5QH, United Kingdom, **5** Ophthalmology, Dept. Organi di senso, University of Rome "Sapienza", Rome, Italy

☯ These authors contributed equally to this work.
* amicera@gmail.com (AM); s.bonini@unicampus.it (SB)

Citation: Micera A, Stampachiacchiere B, Di Zazzo A, Sgrulletta R, Cortes M, Normando EM, et al. (2015) NGF Modulates trkA^{NGFR}/p75^{NTR} in αSMA-Expressing Conjunctival Fibroblasts from Human Ocular Cicatricial Pemphigoid (OCP). PLoS ONE 10 (11): e0142737. doi:10.1371/journal.pone.0142737

Editor: Andrea Caporali, University of Edinburgh, UNITED KINGDOM

Received: January 16, 2015

Accepted: October 26, 2015

Published: November 16, 2015

Data Availability Statement: All relevant data are within the paper.

Funding: This work was supported by the Italian Ministry of Health (MoH) and by the intramural financial support (Fondazione Roma). The funders had no role in study design, data collection and analysis, decision to publish, or preparation of the manuscript.

Competing Interests: The authors have declared that no competing interests exist. In addition, the authors would like to underline that the results

Abstract

Objective

In a previous study, we reported the upregulation of Nerve Growth Factor (NGF) and trkA^{NGFR} expression in Ocular Cicatricial Pemphigoid (OCP), an inflammatory and remodeling eye disease. Herein, we hypothesize a potential NGF-driven mechanism on fibroblasts (FBs) during OCP remodeling events. To verify, human derived OCP-FBs were isolated and characterized either at baseline or after NGF exposure.

Materials and Methods

Conjunctival biopsies were obtained from 7 patients having OCP and 6 control subjects (cataract surgery). Both conjunctivas and primary FB cultures were characterised for αSMA, NGF and trkA^{NGFR}/p75^{NTR} expression. Subcultures were exposed to NGF and evaluated for αSMA, NGF, trkA^{NGFR}/p75^{NTR} expression as well as TGFβ1/IL4 release. For analysis, *early and advanced* subgroups were defined according to clinical parameters.

Results

OCP-conjunctivas showed αSMA-expressing FBs and high NGF levels. A*dvanced* OCP-FBs showed higher αSMA expression associated with higher p75^{NTR} and lower trkA^{NGFR} expression, as compared to *early* counterparts. αSMA expression was in keeping with disease severity and correlated to p75^{NTR}. NGF exposure did not affect trkA^{NGFR} levels in *early* OCP-FBs while decreased both αSMA/p75^{NTR} expression and TGFβ1/IL4 release. These effects were not observed in *advanced* OCP-FBs.

reported in the present manuscript are original and not submitted elsewhere.

Conclusions

Taken together, these data are suggestive for a NGF/p75^{NTR} task in the potential modulation of OCP fibrosis and encourages further studies to fully understand the underlying mechanism occurring in fibrosis. NGF/p75^{NTR} might be viewed as a potential therapeutic target.

Introduction

The Ocular Cicatricial Pemphigoid (OCP) is an immune-mediated chronic inflammatory disease of the eye, characterized by chronic-recurrent conjunctival inflammation, progressive subepithelial fibrosis and tissue remodeling [1–3]. Inflammatory infiltrates and activated Fibroblasts (FBs) contribute actively to the uncontrolled extracellular matrix (ECM) deposition (remodeling process), leading to structural and functional changes (keratinization and blindness) [3,4]. Several pro-inflammatory/fibrogenic cytokines and growth factors, including Transforming Growth Factor β1 (TGFβ1) and Interleukin 4 (IL4), have shown the ability to modulate the survival of activated FBs and their collagen deposition [2,5–7].

An involvement of Nerve Growth Factor (NGF) pathway in OCP has been previously reported by our group: an increased trkA^{NGFR} immunoreactivity has been observed in OCP conjunctival stroma and a consistent NGF release has been quantified in OCP tears [8,9]. The effect of NGF in tissue remodelling and fibroblast activity is actually controversial: NGF might exert pro/anti-inflammatory effects or profibrogenic activity, acting as a "modulator" of the local immune/inflammatory response, in a receptor expression dependent manner [10–16]. In the last decade, the NGF modulatory effect on Fibroblasts (FBs) and their activated myofibroblast counterpart (myoFBs) has been prospected in view of the surface trkA^{NGFR}/p75^{NTR} rate expression and the NGF ability to trigger apoptosis in FBs from different tissues as well as TGFβ1-induced myoFBs [17–21].

To address the question as whether NGF might modulate OCP-fibrosis, activated FBs and NGF immunoreactivity were verified both in tissues and cultures. Next, the study was extended to the *in vitro* characterization of OCP-FBs and the potential NGF influence on OCP-FB phenotype by monitoring αSMA, trkA^{NGFR}/p75^{NTR} and TGFβ1/IL4 in NGF-exposed OCP subcultures.

Materials and Methods

Ethics Statement

The study followed the guidelines of the Declaration of Helsinki for research involving human subjects and was approved by the intramural Ethical committee (UCBM). Informed written consent was signed by each patient adhering to the study.

Patients and conjunctival specimens

Conjunctival biopsies were obtained from 7 patients with clinical and histological (Hematoxylin & Eosin, HE; Bio-Optica, Milan, Italy) diagnosis of OCP (2M/5F; mean age, SD, range 55–88 years) and from 6 healthy age matched patients (control group), during routine cataract surgery (5M/1F; mean age, SD, range 59–81 years).

Two fragments were produced from each biopsy: one conjunctival fragment was included in paraffin and sectioned to provide 5μm-sections for light/confocal microscopy, while the other fragment was used to achieve primary culture of conjunctival OCP FBs.

OCP specimens were classified according to the stage of the disease [22,23] and grouped as follows: early group comprising 3 patients (stages I or II; Foster) and advanced group including 4 patients (stages III or IV). The immunofluorescent analysis was performed for identifying the presence of a linear immunoglobulin deposition alongside the Basament Membrane Zone (BMZ), according to the specific immunoreactivity (FC-coupled IgGAM antibodies; OBT0119F; Oxford Biotech., Oxford, UK), univocally present in OCP positive sections. Basal histology included Giemsa (48900; Fluka, Milan, Italy), Haematoxylin and Eosin (HE; 05-M06014/05-M10002;Bio-Optica; Milan, Italy) as well as the Periodic Acid Schiff (PAS; 04-130802/05-M06002; Bio-Optica; Milan, Italy) stainings.

All sterile tissue culture plastic-ware and reagents were from NUNC (Roskilde, Denmark) and Serva (Heidelberg, Germany). Culture media and supplements were from Euroclone (Milan, Italy). Ultrapure/RNAse free water was provided by Direct-Q5 Apparatus (Millipore, Vimodrone, Milan, Italy).

Explants, FB subcultures and NGF studies

Conjunctival fragments were put as explants in 24-well plates and left to attach for 10min before adding DMEM supplemented with 10% heat-inactivated Fetal Bovine Serum (FBS), 1mM sodium Pyruvate, 2mM glutamine, 100U/mL penicillin and 100μg/mL streptomycin (37°C, 5% CO_2 in air) [17,18]. Outgrowing FBs were quickly harvested (0.2% trypsin-0.025% EDTA; HyQ trypsin; HyClone, Waltham, MA) and directly used or sub-cultured in T-21cm^2/T-75cm^2 flasks (3rd-5th passage) for NGF exposure. The cell culture purity was estimated by the CK19 exclusion test (anti-cytokeratin 19 conjunctival epithelial marker, 1/100; Dako, Hamburg, Germany).

For stimulation studies, serum starved confluent monolayers were exposed to increasing NGF concentrations (0 to 100ng/mL β-NGF Grade I; Alomone Labs Ltd, Jerusalem, Israel) or 1ng/mL TGFβ1 (positive control; R&D system, Minneapolis, MN) performed in 0.5% FBS-DMEM for 24hrs.

Conditioned media were collected for ELISA/Western Blot analysis, while monolayers were directly processed for confocal analysis or treated with trypsin-EDTA solution to obtain single cells for molecular (10^5 cells) / biochemical (10^6 cells) analysis.

Confocal Analysis

Conjunctival sections and monolayers were subjected to fluorescent immunostaining. Briefly, de-waxed sections and confluent monolayers on round coverslips (Mierfield, USA) were washed in Hank's Balanced Sodium Salt (HBSS), fixed in 2% buffered ρ-Formaldehyde (PFA), equilibrated in PBS [10mM phosphate buffer and 137mM NaCl; pH 7.5], briefly permeabilized with 0.5% Triton X100 in PBS (TX-PBS) and probed with the specific antibodies, either alone or in combination: mouse anti-human αSMA antibodies (1/60; Novocastra, Newcastle, UK), goat anti-human NGF antibody (sc-549; 1/100); rabbit anti-human trkA^{NGFR} (sc-118; 1/150) and goat anti-human p75^{NTR} (sc-6188; 1/75) antibodies (all from Santa Cruz Biotech., Santa Cruz, CA). The specific binding was detected by using Cy2/Cy3-conjugated specie-specific secondary antibodies, depending on the specific staining (1/500-1/700; Jackson ImmunoResearch Labs., Europe Ltd, Suffolk, UK). Nuclei were counterstained with Propidium Iodide (5μg/mL; ICN, Milan, Italy). Acquisitions were carried out using the E2000U confocal microscope equipped with C1 software (Nikon, Tokyo, Japan). Control sections were stained in parallel (control irrelevant IgGs; Vector Laboratories, Inc. Burlingame, CA) and used for the channel-series acquisitions (Nikon).

Flow cytometry

Single-cells were washed in HBSS containing Ca^{++}/Mg^{++} and fixed in 3.7% buffered PFA. After washing, cells were either directly immunostained or further incubated in 70% methanol in PBS (20°C, 24hrs). For staining, cells were equilibrated in FACS buffer [0.1% saponin and 0.1% NaN_3 in PBS; pH 7.5] and incubated with the above reported primary antibodies diluted in 0.1% BSA-FACS buffer. The specific binding was detected with Cy2/PE-conjugated specie-specific secondary antibodies (1/600-1/700; Jackson). Cells (10^4 events) were analysed using the MACSQuant flow cytometer and cell plots were arranged using the manufacturers' provided software (Miltenyi Biotech., Gladbach, Germany). Changes in Mean Fluorescence Intensity (MFI) were calculated as follows: $\Delta MFI = [(MFI_{specific}/ MFI_{not\text{-}specific}]$ and ΔMFI values ≥ 1 were used for statistical analysis.

Relative Real-Time PCR analysis

Total RNA was extracted from confluent monolayers using the Puregene RNA purification kit (Gentra Systems, Minnesota, USA). Total RNA samples were spectrophotometrically analysed (ND-1000; NanoDrop, Wilmington, DE; $\lambda_{260}/\lambda_{280} > 1.8$). Total RNA (3 μg) samples were reverse transcribed to a final volume of 21μlL, using 50 pM oligo dT21-primer, 1 mM dNTP mix and 200 U reverse transcriptase (IMPROM; Promega, Milan, Italy) in a programmable PTC100 thermocycler (MJ Research, Watertown, MA) and 3μL were run for amplification with the specific target/referring primers in an Opticon2 MJ thermocycler (MJ Research), according to the manufacturers' instructions (Table 1). PCR experiments were carried out in a final volume of 20μL containing 3μL cDNA for target genes (or 1μL/3μL for GAPDH/H3 reference genes) and 17μL of master mix [10μL SYBR Green PCR Mix (Applied Biosystems, Foster City, CA), 0.5μL of each primer (10 pM; MWG, Biotech, Ebersberg, Germany) and milliQ-water]. Amplicons were verified for their specificity according to the Southern blotting analysis. Negative controls (without template or with total RNA) were carried out for each run, to rule out any genome contamination. Single threshold cycle values (Cts) were run in the REST 384–2006 software [24] to get increase or decrease difference in target gene expression, with respect to reference genes and compared to controls. Data are gene expression ratio provided in log2 scale.

ELISA

To evaluate NGF in the culture media, a two site NGF-ELISA (0.5pg/mL sensitivity and no cross-reactivity) was carried out in Maxisorp NUNC 96 well ELISA plates precoated with mouse anti-NGF antibodies (0.4μg/mL; MAB256, R&D) and incubated with standards (0.15pg/mL to 1ng/mL β-NGF; Alomone) or prediluted samples (1:3). The following steps included as follows: the biotinylated polyclonal anti-NGF antibodies (0.15μg/mL; BAF256, R&D), the streptavidin solution (Biosource International, Camarillo, CA) and the TMB substrate (Biosource). Optical density was detected by an ELISA plate reader ($\lambda_{450-550}$; Sunrise; Tecan Systems, Inc., San Jose, CA) and calculations were carried out according to the protein normalization (A280 Nanodrop) [16]. The biological activity of NGF released by OCP-FBs was verified separately by using a PC12 bioassay (see [18]).

TGFβ1 and IL4 were measured in the conditioned media by commercially available ELISA kits, according to the manufacturers' instructions (Biosource).

Western Blotting

Total proteins were extracted from single-cells lysed in modified RIPA buffer [50 mM Tris-HCl (pH 7.7), 150mM NaCl, 1%Triton X-100 and 0.1% SDS] freshly supplemented with

Table 1. Primers and amplification program used in the study.

Primer	Sequence	bp	Ta*	Accession number
NGF	for 5'-CTG GCC ACA CTG AGG TGC AT-3'	120	55°C, 30sec	**BC011123**
	rev 5′ -TCC TGC AGG GAC ATT GCT CTC-3′			
trkA^{NGFR}	for 5'-CAT CGT GAA GAG TGG TCT CCG-3'	102	57°C, 25sec	**M23102**
	rev 5'-GAG AGA GAC TCC AGA GCG TTG AA-3'			
p75^{NTR}	for 5'-CCT ACG GCT ACT ACC AGG ATG AG-3'	147	57°C, 25sec	**AF187064**
	rev 5′ -TGG CCT CGT CGG AAT ACG-3′			
αSMA	for 5'-GAA GGA GAT CAC GGC CCT A-3'	125	55°C, 30sec	**BC017554**
	rev 5′ -ACA TCT GCT GGA AGG TGG AC-3′			
TGFβ1	for 5'-TCC TGG CGA TAC CTC AGC AA-3'	110	57°C, 25sec	**BC017288**
	rev 5′ -GCC CTC AAT TTC CCC TCC AC-3′			
GAPDH	for 5'-CCT GAC CTG CCG TCT AGA AA-3'	111	55°C, 30sec	**BC013310**
	rev 5′ -ACC TGG TGC TCA GTG TAG CC-3′			
H3	for 5′ -GCT TCG AGA GAT TCG TCG TT-3′	113	59°C, 30sec	**NM005324**
	rev 5′ -GAA ACC TCA GGT CGG TTT TG-3′			

The amplification program was as follows: 95°C/15min, followed by 47 cycles of denaturation at 94°C/15sec, annealing Ta* at 25sec or 30sec, extension at 72°C/15sec. Melting curves for each specific primer were monitored between 60°C–90°C, at the end of amplification, before a further extension at 75°C/5min. In bold, referring gene details;
*Ta, annealing temperature; bp, base-pairs of amplicons.

doi:10.1371/journal.pone.0142737.t001

phosphatase/protease inhibitors (Pierce). Equivalent amounts of protein (30μg) were subjected to 7–15% SDS-PAGE electrophoresis (Miniprotean3; Bio-Rad, Hercules, CA) and resolved proteins were transferred to Hy-bond membranes (semi-dry blotting apparatus; Bio-Rad). The membranes were washed in 0.05% Tween 20 in PBS (TW-PBS), blocked in 5% non-fat dry milk-PBS and probed with trkA^{NGFR} (1/700), p75^{NTR}(1/500), αSMA (1/500) and GAPDH (1/1000) primary antibodies, followed by secondary POD-conjugated specie-specific antibodies (1/10000; Jackson Immuneresearch). Developing was performed according to the ECL technique (SuperSignal West Pico Trial; Pierce, Rockford, IL). Bands were acquired/analysed in a Kodak Image station equipped with a 1D Image analysis software (110F; Kodak, Tokyo, Japan).

Statistical Analysis

All experimental procedures were conducted in triplicate, each one repeated three times. Both molecular and biochemical data (means±SD) were analysed for significant differences ($p < .05$), by the ANOVA-Tukey-Kramer coupled post-hoc analysis (StatView II for PC; Abacus Concepts. Inc., Barkley, CA). REST-ANOVA analysis followed by Tukey Kramer posthoc comparisons was used to validate molecular data.

Results

Only conjunctival biopsies from patients' with confirmed ophthalmic and microscopic diagnosis of OCP were included in this study. Immunofluorescent staining revealed the presence of a clear linear fluorescence alongside the BMZ, representative of autoantibodies deposition in both *early* (A) and *advanced* (B) OCP sections (Fig 1). No significant difference in IgGAM immunoreactivity was observed between *early* and *advanced* OCP, except for an increasing fluorescent signal in the epithelium and stroma (asterisk; Fig 1B). Contiguous to those IgGAM staining, basal histology was also performed by using Giemsa (Fig 1C and 1D), HE (Fig 1E and

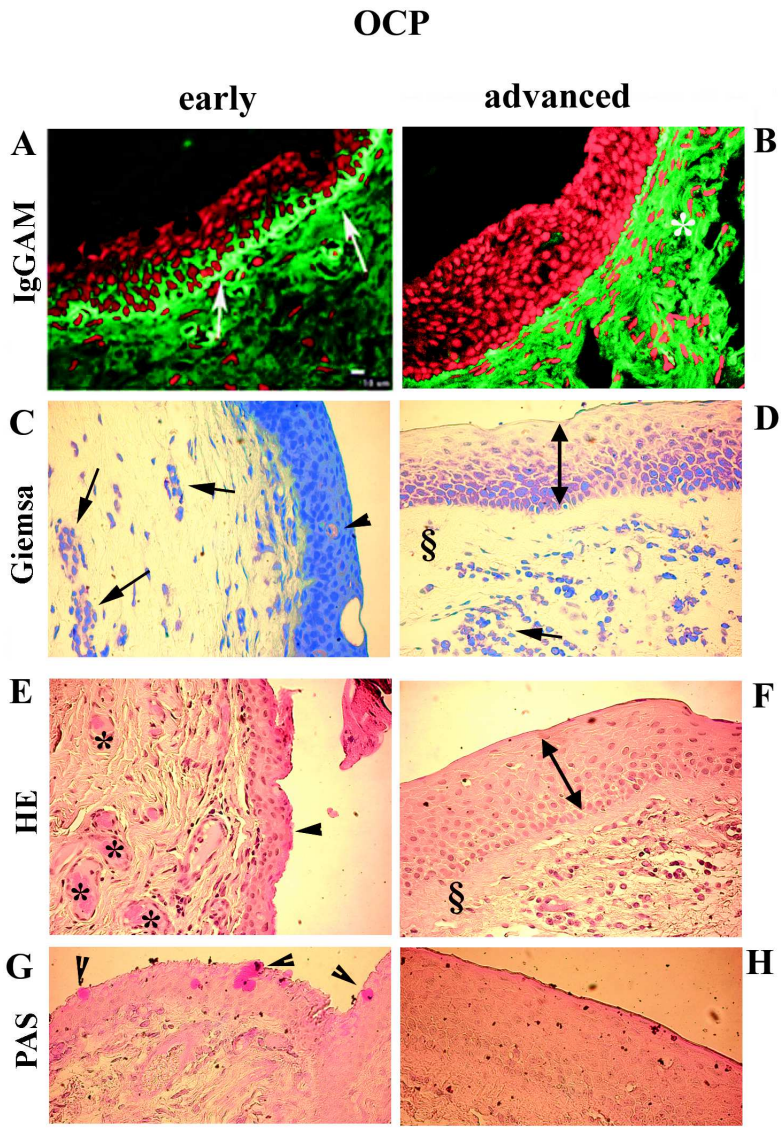

Fig 1. Histological characterization of OCP conjunctivas. Representative confocal (A-B) and light microscopy (C-H) images, including Giemsa (CD), HE (EF) and PAS (GH) stainings, from dewaxed conjunctival sections. A-B. Linear fluorescent-coupled IgGAM reactivity in the Basement Membrane Zone of *early* (white arrows; A) and *advanced* (B; the white asterisk indicates the stromal immunoreactivity) OCP sections. Fluorescent linear immunoreactivity is absent in normal sections. Depletion of goblet cells (pointed by black arrowheads) in *early* (C,E,G) with respect to the complete absence in *advanced* OCP (D,F,H); the presence of a squamous metaplasia (↔) particularly in *advanced* OCP (D,F); vessel ectasia (*) more prominent in *early* (E) than *advanced* (F); edema with mild infiltrates (arrows) in *early* (C) and to a less extend in *advanced* (D) OCP, particularly plasmacells and some granulocytes; and finally superficial homogenization of connective tissue (§), particularly evident in *advanced* OCP (D,F). Magnifications: x400.

doi:10.1371/journal.pone.0142737.g001

1F) and PAS (Fig 1G and 1H). A depletion of goblet cells was observed in *early* OCP (arrowheads) while the absence of goblet cells was detected in *advanced* OCP, as pointed in Giemsa, HE and particularly PAS panels (Fig 1C–1H). The presence of squamous metaplasia (pluristratified non-keratinised epithelial with absence of goblet cells and homogenization of connective tissue) was particularly evident in *advanced* OCP (see § in Fig 1D and 1F). A marked vessel

ectasia was particularly evident in *early* OCP (see asteriks in Fig 1E). Edema and mild infiltrates with prevalence of plasmacells (arrows) were observed in *early* with respect to *advanced* OCP (Fig 1C).

Characterization of activated FBs

Adjacent conjunctival sections and primary cultures of FBs were analysed for αSMA expression by confocal microscopy and flow cytometry (FCM) analysis. As shown in Fig 2, αSMA immunoreactivity in outgrowth of OCP-tissue (B) and outgrew FBs (D), as compared to control specimens (respectively A and C; $p < .05$). FCM analysis confirmed the higher αSMA protein expression in OCP-FBs (Fig 2E; $p < .05$). FCM results were corroborated at the molecular level (+14.00±4.80 expression ratio in OCP-FBs *vs*. controls; $p < .05$).

Expression of NGF and trkA^{NGFR}/p75^{NTR}

OCP conjunctiva and OCP-FBs were examined for NGF-trkA^{NGFR}/p75^{NTR} expression. As observed by confocal analysis, NGF expression was decreased in the epithelium and specifically increased in OCP stroma, as compared to controls (Fig 3A and 3B; $p < .05$). Indeed, confocal analysis showed higher cytoplasmic and perinuclear NGF immunoreactivity in outgrew OCP-FBs, supporting those data observed in OCP stroma (see arrows; Fig 3C). In addition, the conditioned media from OCP-FBs showed higher NGF levels than those of control counterparts (420.00±90.00 *vs*. 220.00±64.00 pg/mL; $p < .05$), as detected by NGF ELISA. In line, NGFmRNA was increased in these OCP-FBs, as compared to their control FBs (+5.00±1.30 expression ratio; $p < .05$). No significant difference was quantified between *early* and *advanced* specimens.

Confocal analysis showed a high p75^{NTR} expression associated with a weak trkA^{NGFR} expression in OCP-FBs (Fig 4B). By contrary, control FBs showed a huge trkA^{NGFR} expression with respect to p75^{NTR} slightly expressed (Fig 4A). To support, the related FCM analysis for trkA^{NGFR} and p75^{NTR} are provided in Fig 4C and 4D respectively.

αSMA and p75^{NTR}co-expression in OCP-derived activated FBs

The higher αSMA and p75^{NTR} and the lower trkA^{NGFR} protein expressions in OCP-FBs were also detected by WB analysis, as compared to control FBs (Fig 5A; $p<0.05$). As shown in Fig 5B, αSMA protein co-localized with p75^{NTR} but not with trkA^{NGFR}, as detected by confocal analysis. This would suggest the existence of a specific trkA^{NGFR}/p75^{NTR} expression ratio during the progress of fibrosis. Particularly, basal histology showed a strong infiltration of inflammatory cells (arrows pointing to plasmacells in Fig 1C), the presence of connective tissue homogenization (asterisk in 1D and 1F) in the underlying stroma (§) and a significant decrease (absence) of goblet cells in the epithelium of *advanced* OCP sections (see arrowheads pointing residual goblet cells in *early* OCP) (Fig 1C and 1E). Activated fibroblast were also visible in *early* OCP (Fig 1C). No significant difference in αSMA, p75^{NTR} and trkA^{NGFR} transcripts was detected in *early* OCP-FBs compared to controls (respectively +1.05±05, +1.30±0.50 and +2.00 ±1.00 expression ratio; $p>.05$). In *advanced* OCP-FBs, αSMA and p75^{NTR} transcripts were significantly increased (+9.00±0.40 and +5.00±0.50 expression ratio; $p < .001$) while trkA^{NGFR} transcript was significantly decreased (-4.00±1.00 expression ratio; $p < .05$), as compared to controls. By FCM analysis, αSMA protein was increased in *early* OCP-FBs (2.8±0.58 *vs*. 0.22 ±0.06 MFI, early *vs*. controls; $p>.05$) and significantly increased in *advanced* OCP-FBs (27.05 ±3.6 *vs*. 0.22±0.06 MFI, advanced *vs*. controls; $p < .001$). Indeed, p75^{NTR} protein was increased in both *early* (15.52±5.97 *vs*. 1.44±0.6 MFI, early *vs*. controls; $p < .05$) and *advanced* (17.0±3.0 *vs*.1.44±0.6 MFI, advanced *vs*. controls; $p < .01$) OCP-FBs. Finally, trkA^{NGFR} protein

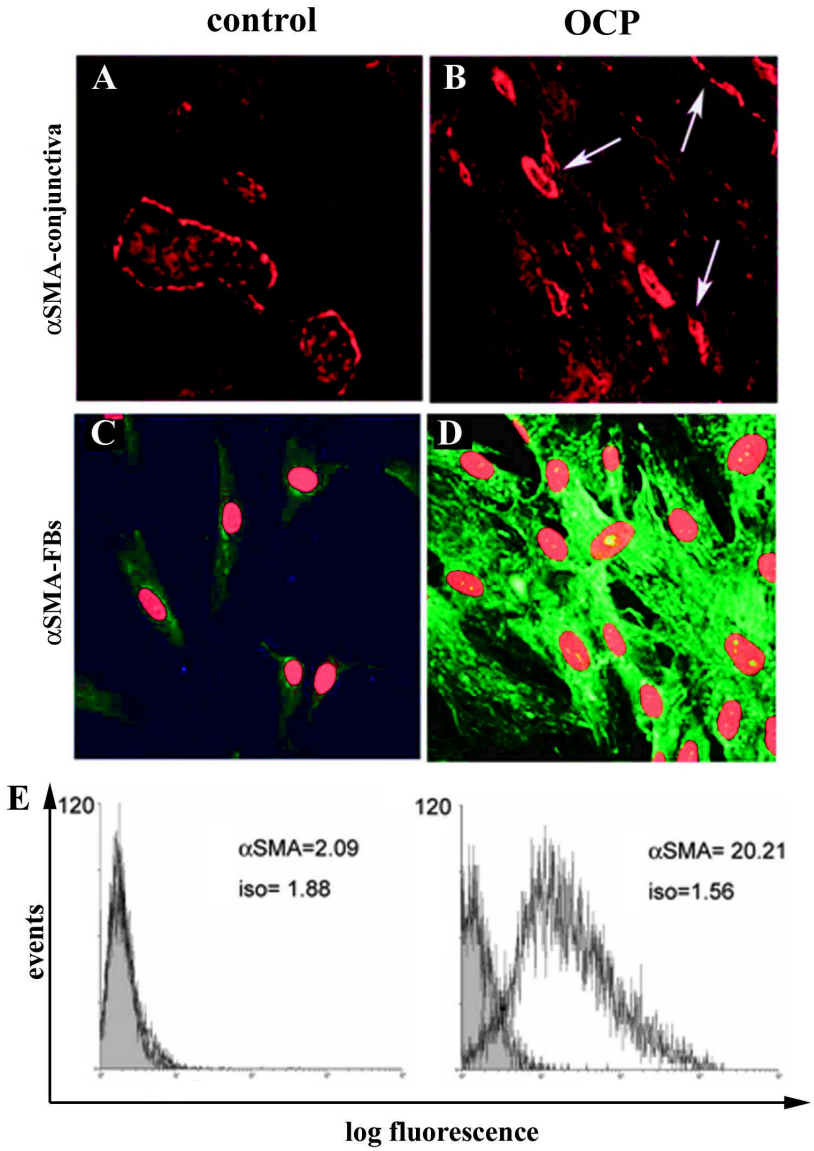

Fig 2. aSMA expression in both OCP conjunctiva and derived FBs. A-D. Confocal analysis for α-SMA in both control (A) and OCP (B) conjunctival biopsies, as well as in control (C) and OCP (D) FB. Arrows point to specific α-SMA immunoreactivity in OCP tissue (B; red staining; see M&M for details). In monolayers, nuclei were counterstained with propidium iodide (C-D). [Magnifications: AB, x400; CD, x600] E-F. Flow cytometry analysis specific for α-SMA in control (E) and OCP (F) FBs. iso = fluorescence intensity related to isotypes.

doi:10.1371/journal.pone.0142737.g002

expression in *early* OCP-FBs was comparable to those of control-FBs while it decreased in *advanced* OCP-FBs (2.41±1.27 *vs*. 15.5±1.00 MFI, *advanced vs*. controls; $p < .01$).

NGF modulation of αSMA and trkA^{NGFR}/p75^{NTR}expression in OCP-FBs

NGF effect on αSMA and trkA^{NGFR}/p75^{NTR} modulation was thereafter investigated by exposure to 10ng/mL NGF over 24hrs. A preliminary dose response study was carried out on OCP-FBs (0–100 ng/mL NGF over 24hrs), highlighting the 10 ng/mL NGF dosage. In *early* OCP-FBs, decreased αSMA and p75^{NTR} (respectively 0.83±0.19 *vs*. 2.8±0.58 MFI and 1.08